

Miniaturized ultraviolet sources driven by dielectric barrier discharge and runaway electron preionized diffuse discharge

MIKHAIL EROFEEV^{1,2*}, EUGENII BAKSHT¹, VICTOR TARASENKO^{1,2}

¹Institute of High Current Electronics, Akademicheskoy Avenue 2/3, 634055 Tomsk, Russia

²National Research Tomsk Polytechnic University, Lenina Avenue 30, 634050 Tomsk, Russia

*Corresponding author: mve@loi.hcei.tsc.ru

In this work we have studied the energy and spectral characteristics of miniaturized dielectric barrier discharge KrCl-, XeCl-, XeBr-, and Xe₂-excilamps of various designs as well as short pulse point-like light sources based on runaway electron preionized diffuse discharge. The maximum ultraviolet power density was 20 mW/cm², which is comparable with the densities of ordinary dielectric barrier discharge excilamps, whereas the maximum efficiencies of the excilamps were not greater than 2.5%. The causes for the low radiation efficiency of the compact dielectric barrier discharge driven excilamps were analyzed. It is found that at an electron concentration of $n_e > 10^{14} \text{ cm}^{-3}$, the efficiency decreases due to enhanced quenching of excited atoms or molecules in dissociation by electron impact. The spectral characteristics of a runaway electron preionized diffuse discharge formed between two pointed electrodes in atmospheric pressure air in an inhomogeneous electric field at a gap shorter than 8 mm were investigated. It is shown that the radiation spectrum of the discharge consists of bands of the second positive nitrogen system, and as the discharge transforms to a spark, lines of the electrode material appear in the spectrum. At a gap of 0.5 mm, weak X-rays from the discharge gap were detected.

Keywords: excilamps, light sources, plasma spectroscopy, runaway electron preionized diffuse discharge.

1. Introduction

The incoherent spontaneous ultraviolet (UV) sources based on the fluorescence of decaying rare gases molecules and their halides in dielectric barrier discharge (or DBD excilamps) have been intensively studied in the last 20 years and high efficiencies (tens of percent) and radiation powers (kW) have been attained [1–4]. The average radiation power of the gas discharge plasma is increased by increasing the interelectrode gap d and/or the electrode area, which is well described by similarity laws. By this time, there have been designed high-power and efficient UV sources, which is interesting for applications dealing with surface cleaning [5, 6], microelectronics [7], microbiology [8, 9], ecology [10], and for research purposes such as calibration of optical system [11].

However, spectroscopy, ion sources of mass spectrometers, and devices for quantitative analysis require miniature gas discharge UV sources which have the same specific power densities as ordinary DBD sources and provide spatially stable radiation output in a wide pressure range. The miniaturization will provide lower power consumption of the sources and make their practical use simpler and wider. In practice, the miniaturization of the sources by decreasing the interelectrode gap and increasing the operating pressure under the same discharge excitation conditions faces a series of problems associated with violation of the similarity laws. As the gas pressure is increased up to hundreds of torrs, the discharge characteristics start being much affected by the loss of electron's energy due to decreasing of its free path. That leads to increasing voltage, and, as a consequence, overheating and spurious reactions the rate of which increases with the temperature. This impairs the discharge operation, or causes its contraction, or the discharge is not ignited at all. High radiation powers at increased pressures and small gaps with no preionization can be attained with the use of nanosecond high-voltage discharges in an inhomogeneous electric field [12, 13]. At macro- and microprotrusions of the cathode surface, the electric field is amplified tens times. The electric field near the surface can thus reach critical values at which initiating electrons turn to the so-called runaway mode (when the electrons in the applied electric field gain more energy than they lose in collisions) and generate slow electrons; this gives rise to avalanches and their overlapping, and eventually provides a volume discharge [14]. It was proposed to term this type of discharge a runaway electron preionized diffuse discharge (REP DD) [15].

By now, there have been designed UV and VUV sources based on a REP DD [16, 17] excited by the RADAN nanosecond high-voltage generators [18]. With the RADAN-150 generator, the UV radiation pulse width for DBD-driven XeCl-, KrCl-, XeBr-, and KrBr-excilamps was 4 ns at a peak radiation power density of up to 700 W/cm^2 [19]. Energy characteristics of REP DD in pulse repetition mode have been studied in [20]. However, for designing miniature sources, the emitting volume and the generator voltage should be decreased.

The objective of the work is to study the energy and spectral characteristics of spontaneous UV radiation of the plasma of a barrier discharge and runaway electron preionized diffuse discharge at small interelectrode gaps (less than 1 cm) in a wide range of pressures (from tens of torr to atmosphere) of inert gases, their halogenides, nitrogen, and air on microsecond and nanosecond repetitive pulsed generators and to design miniature nanosecond repetitive pulsed UV sources.

2. Experimental setups

The compact DBD-driven emitters were made of quartz tubes of high transparency (no less than 80% at a wavelength of 170–350 nm) and had different designs (Fig. 1) which allowed to arrange coplanar or planar two barrier discharge and single barrier discharge. Excilamp of the coplanar barrier discharge arrangement with one parallel electrode pair located outside a tube of elliptic cross-section is shown in Fig. 1a. In

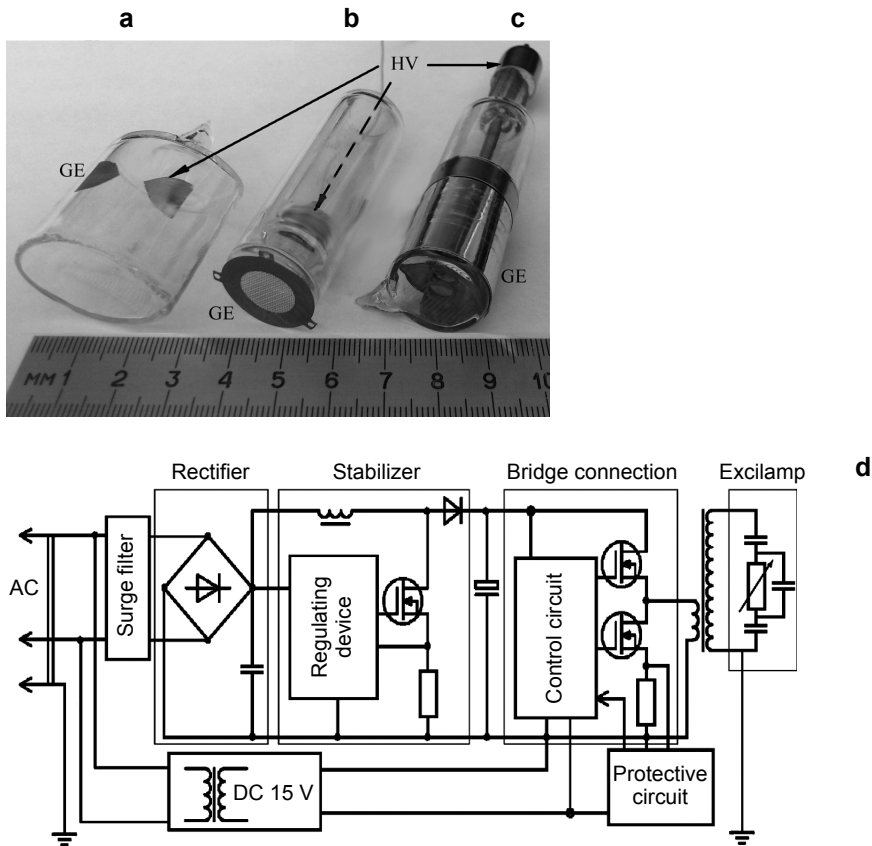


Fig. 1. Design of compact DBD-driven excilamps (a–c) and schematic diagram of the electrical circuit (d).

the planar two barrier excilamp (Fig. 1b) and cylindrical single barrier excilamp (Fig. 1c) with outer quartz tube diameter of 2 cm, the radiation was extracted through the bulb face. The ground electrode (GE) of the coaxial two-barrier planar excilamp (Fig. 1b) was a metal grid placed on the output windows and their high-voltage (HV) electrode was inside the inner tube. The HV electrode of the single-barrier excilamps (Fig. 1c) was either a steel spiral or a tungsten core of diameter 1 mm. Dielectric barrier discharge was formed in rare gases, their mixtures with halogens and in Ar-N₂ mixture. The highest radiation power densities of compact excilamps was attained on Xe₂^{*}, KrCl^{*}, XeCl^{*}, XeBr^{*} and N₂ molecules. The discharge gap d was ~8 mm for all excilamp designs.

The solid electrodes were made of Al:Mg foil and had an area of 1–5 cm²; the perforated ground electrodes were metal grids of transparency 60%. The working mixtures were prepared directly in the excilamp bulbs.

The radiation power densities were determined using calibrated HAMAMATSU H8025 photodetectors with a maximum spectral sensitivity at 222 and 172 nm. The compact excilamps were excited by unipolar and bipolar voltage generators with a pulse

repetition frequency variable from 10 to 300 kHz. The voltage pulse amplitude was 3–12 kV. Figure 1d shows the schematic diagram of the electrical circuit of the generator loaded with two barrier excilamp described in [4]. In studies of the single-barrier Xe₂-excilamps, we also used a high-voltage generator producing voltage pulses of FWHM 7.5 μ s, 1.5 μ s, 250 ns, and 100 ns and amplitude \sim 20 kV at a pulse repetition frequency from 340 to 1200 Hz.

The single-barrier N₂-excilamps were excited by a generator with a voltage pulse amplitude in the transmission line of up to 12.5 kV at a pulse repetition frequency of 370–1050 Hz, FWHM of the voltage pulse of about 1 ns, and pulse rise time of about 0.2 ns at a level of 0.1–0.9 (FPG-10 generator, FID GmbH).

Volume discharges in atmospheric pressure air were formed between two electrodes of small curvature radius (pointed electrodes). The electrode material was stainless steel, aluminum, copper, titanium, tantalum, niobium, and tungsten. The stainless steel electrodes were standard medical needles of outer diameter 0.5 mm; the other electrodes were made of foils of the above materials. The study was performed with gaps of 0.5, 1, 2, and 3 mm with FPG-10 generator.

The excilamp current and voltage were measured with current shunts, voltage dividers, and Tektronix TDS-3034 and DPO70604 oscilloscopes (6 GHz, 25 GS/s). The time dependence of radiation pulses was measured with a Photek PD025 Low Noise S20 photodiode. The excilamps' radiation spectra were measured by a StellarNet EPP2000-C25 spectrometer (operating band 200–850 nm, spectral half-width of instrument function no more than 1.5 nm) and calibrated Ocean Optics B.V. HR4000 spectrometer (operating band 200–300 nm). Photos of the discharge glow were taken with a Sony A100 digital camera and a HSFC-PRO CCD camera.

3. Results and discussion

3.1. Miniaturized narrow-band UV emitters driven by a microsecond two-barrier discharge

The working medium of two-barrier excilamps is most often excited by sinusoidal or trapezoidal alternating voltage with an amplitude of several kilovolts and pulse repetition frequency from several to hundreds of kilohertz.

At voltage amplitude of 4 kV with 100 kHz pulse repetition rate, the highest radiation power density of the coplanar barrier discharge excilamps were obtained in mixtures of Kr:Cl₂ = 100:1 and Xe:Br₂ = 18:1 at a total mixture pressure of 57 and 45 torr and were 3 and 7 mW/cm² at a radiation efficiency to the angle 4 π of 2% and 2.5% for the KrCl- and XeBr-excilamps, respectively.

The microdischarge represented a thin channel of diameter \sim 2 mm on the inner emitter surface, diffusely expanding under the electrodes. The position of the discharge relative to the electrodes was invariant with time. This makes it possible to obtain uniformly light-struck regions of size up to 1 cm² at a distance more than 1 cm from the excilamp surface without using additional optical elements.

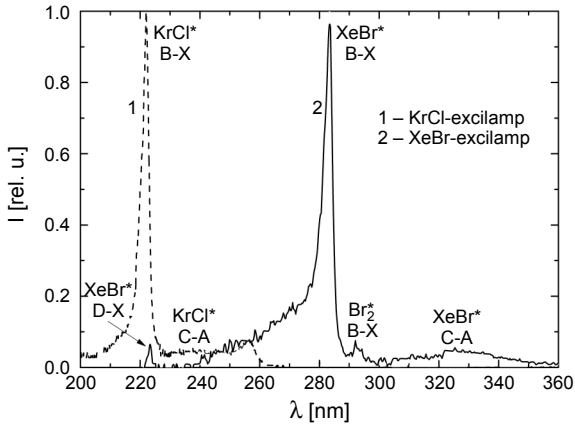


Fig. 2. Radiation spectra of the compact coplanar KrCl- and XeBr-excilamps.

In the mixtures of inert gases with halogens, the radiation of the discharge plasma arises at the transitions between the lower excited levels and ground repulsion level of the exciplex molecules formed at low pressures (less than 100 torr) in harpoon reactions [3] and, at higher pressures, they can also be formed through ion-ion recombination [21] of a positive atomic ion or positive molecular ion of inert gas with a negative halogen ion.

The radiation spectrum of the excilamps under study (Fig. 2) contained *B-X*, *C-A*, and *D-X* transition bands of KrCl^* and XeBr^* molecules but differed somewhat from the spectra of capacitive, glow, and barrier discharge excilamps [22–24]. So in the spectra of the glow and capacitive discharge KrCl- and XeBr-excilamps, the *C-A* and *D-X* transition bands are more pronounced, and in the spectrum of the barrier discharge excilamps, the *D-X* band is almost entirely absent. In the coplanar barrier discharge excilamp, most of the radiation power is concentrated in the *B-X* band of KrCl^* and XeBr^* molecules. The width of this band at half maximum is 3 nm for the KrCl-excilamp and 4 nm for the XeBr-excilamp, which is 1.5 times narrower than that found in the capacitive and glow discharge excilamps [23, 24]. This fact is explained by higher pressures used in the coplanar discharge excilamps. Moreover, the large buffer volume and proximity of the microdischarge to the wall provide better cooling and thus increase the lifetime of this type of excilamps: after 1000-h operation, the excilamp power remained unchanged.

The average electron concentration n_e was estimated by the following formula:

$$n_e = j(e w_{\text{dr}})^{-1} \quad (1)$$

where j is the current density calculated from the oscillograms of the current and voltage, e is the electron charge, w_{dr} is the drift velocity. The electron drift velocities in krypton and xenon at specified electric field strengths and pressures were taken from the reference book [25]. For the KrCl-excilamp, the electron concentration was

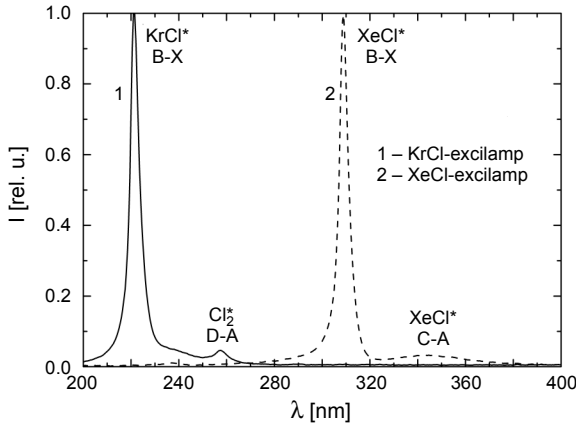


Fig. 3. Radiation spectra of the compact planar KrCl- and XeCl-excilamps.

10^{12} cm^{-3} , and for the XeBr-excilamp, it was 10^{13} cm^{-3} . Note that the obtained electron concentrations n_e were two orders of magnitude lower than the electron concentration typical of a barrier discharge [26] for the same working molecules.

The maximum radiation power densities at the planar lamp's surface are attained in mixtures of Xe/Kr:Cl₂ = 200:1 at a pressure of 145 torr and pulse repetition frequency of 100 kHz and are 20 and 10 mW/cm² for the XeCl- and KrCl-excilamps, respectively. At pressures above 200 torr, the discharge transforms into a spark and its power decreases.

In the planar excilamps, the electric field strength has uniform distribution, and the plasma is dominated by electron collisions with neutrals; hence, the average electron concentration n_e can be estimated by the formula [27]:

$$n_e = 2Pm\nu_c(eE)^{-2} \quad (2)$$

where m and e are the electron mass and charge; ν_c is the electron collision frequency equal to $25 \times 10^9 \text{ Hz/torr}$ in xenon [27]; P is the specific excitation power and E is the maximum electric field strength which are calculated from oscillograms of the current and voltage. At optimum pressures, the electron concentration was $\sim 2 \times 10^{12} \text{ cm}^{-3}$.

The spectra of the KrCl- and XeCl-excilamps (Fig. 3) represent narrow *B-X* bands of the working molecules and weak *C-A* bands whose contribution to the total radiant flux is no more than 4.5%. The radiation pulse width of the excilamps corresponds to the current pulses through the excilamps and lies in the range from several to tens of microseconds depending on the pressure of the working medium.

3.2. Miniaturized narrow-band UV emitters driven by a microsecond single-barrier discharge

The single-barrier excilamps make it possible to form a discharge at higher mixture pressures, thus increasing the formation rate of excimer or exciplex molecules and

the radiation power. However, the metal electrode present in the discharge region, due to halogen-metal reaction, greatly decreases the halogen concentration in the working mixture, and hence, the excilamp lifetime. Therefore, experiments were performed on halogen-free single-barrier Xe_2 -excilamps (Fig. 1c).

At pressures of several and tens of torr, the radiation spectrum of the plasma in the discharge in xenon is dominated by transitions of the first and second continua. The first continuum corresponds to the transitions from high vibrational levels of the state $1_u(3P_2)$ or $0_u^+(3P_1)$ to the dissociative $0_g^+(1S_0)$ ground state of a xenon molecule. The second continuum corresponds to the transitions from low vibrational levels of both molecular states to the ground state. To determine the optimum voltage pulse width, we used a high-voltage generator which produced voltage pulses of amplitude ~ 20 kV and FWHM of 7.5 μs , 1.5 μs , 250 ns, and 100 ns. Varying the voltage pulse repetition frequency of the generator from 10 to 70 kHz made it possible to vary the excitation power deposited to the discharge between 10 and 39 W. The maximum radiation power densities of the single-barrier excilamp were obtained at an excitation pulse width of 1.5 μs and xenon pressure of 300 torr which was the optimum pressure for all excitation modes used. Figure 4 shows the dependence of the radiation power density and efficiency of the single-barrier Xe_2 -excilamp on the power deposited to the discharge.

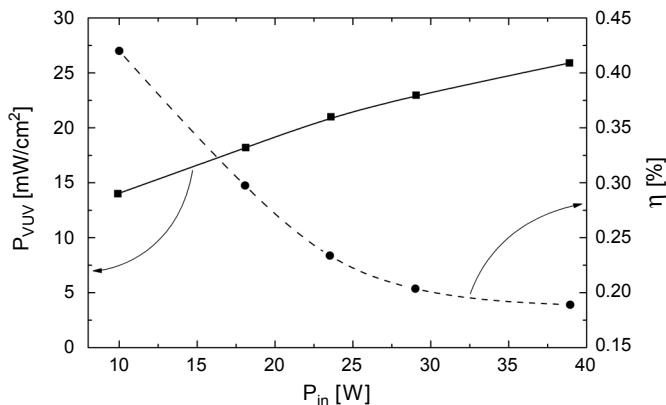


Fig. 4. Radiation power density and efficiency of the single-barrier Xe_2 -excilamp vs. the power deposited to the discharge.

It is seen from Fig. 4 that as the power deposited to the discharge is increased, the radiation power density increases almost linearly; however, the radiation efficiency of Xe_2 molecules decreases. The latter fact is explained by overheating of the working gas and contraction due to the specific excitation power in excess of the optimum values which, according to [28], are ~ 1 W/cm³. The main group of reactions in which energy is released includes elastic collisions, dissociative recombination, predissociation, and collisional association. In this experiment, the specific excitation power was 1.8 and 7.2 W/cm³ at a pulse repetition frequency of 15 and 68 kHz, respectively. The electron

concentration calculated by formula (2) for these specific excitation powers was 4.2×10^{13} and $1.8 \times 10^{14} \text{ cm}^{-3}$, respectively. The increase in n_e also causes a decrease in radiation efficiency due to enhanced quenching of excited xenon atoms in dissociation reactions by electron impact. Moreover, as shown [29], the rates of three-particle formation of $\text{Xe}_2[0_u^+(^3P_1)]$ and $\text{Xe}_2[1_u(^3P_2)]$ molecules with high vibrational states are equal to $\alpha_{31} = 3.90 \times 10^{-27} \text{ T}^{-1.78} \text{ cm}^{-6} \text{ s}^{-1}$ and $\alpha_{32} = 1.34 \times 10^{-27} \text{ T}^{-1.70} \text{ cm}^{-6} \text{ s}^{-1}$, *i.e.*, these rate decrease with increasing gas temperature.

The radiation spectrum of the compact single-barrier Xe_2 -excilamps at the optimum pressures represents a band with a maximum at 172 nm and does not differ as a whole from the radiation spectra of conventional DBD-driven Xe_2 -excilamps.

3.3. Miniaturized narrow-band UV emitters driven by a nanosecond single-barrier discharge

Single-barrier excilamps allow a gap breakdown at lower voltages compared to two-barrier excilamps, all other things (pressure, components ratio in gas mixture, interelectrode gap) being equal. Moreover, decreasing the excitation pulse width and rise time to several and tens of nanoseconds makes it possible to realize a volume discharge at higher voltages and mixture pressures, and this increases the radiation power and decreases the radiation pulse width.

Experiments were performed on the single-barrier excilamp (Fig. 1c) with a pointed tungsten cathode. The working medium was nitrogen, nitrogen-argon mixtures, air, and xenon. Figure 5a shows the dependences of the radiation power density in pure N_2 (curve 1), $\text{Ar}:\text{N}_2 = 50:1$ (curve 2), and $\text{Ar}:\text{N}_2 = 200:1$ (curve 3) for the FPG-10 generator operating at voltage pulse amplitude of 12 kV. The highest energy characteristics were obtained in the nitrogen-argon mixtures in which excitation of the $C^3\Pi_u$ state of a nitrogen molecule from its ground state can proceed not only by electron impact

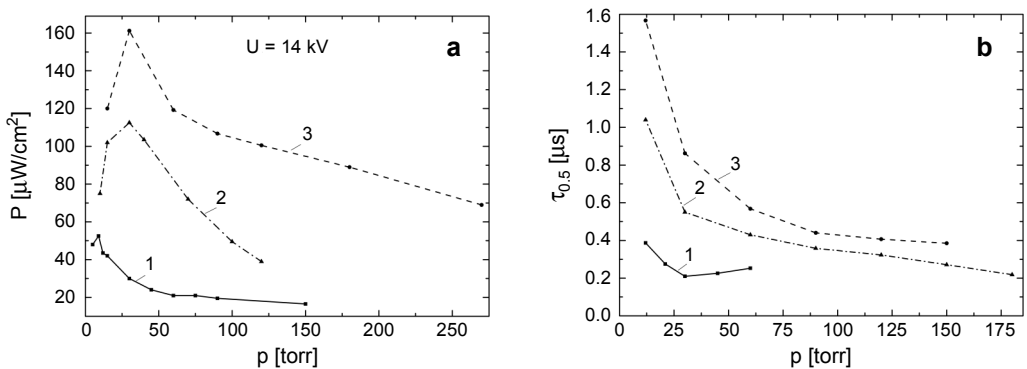


Fig. 5. Radiation power density (a) and its pulse width (b) of the single-barrier N_2 -excilamp vs. working mixture pressure: pure nitrogen (curve 1), $\text{Ar}:\text{N}_2 = 50:1$ (curve 2), and $\text{Ar}:\text{N}_2 = 200:1$ (curve 3) at excitation pulse amplitude $U = 12.5 \text{ kV}$.

(whose efficiency is low), but also through resonant energy transfer from metastable levels of an argon atom. At a low nitrogen percentage ($\sim 1.5\%$) in the N_2 -Ar mixture, most of the energy deposited to the plasma is expended in excitation of the lower levels of argon and in its ionization and is then transferred to nitrogen molecules. Therefore, in the optimum mixtures, the partial pressure of argon is much higher than the partial pressure of nitrogen. The maximum radiation power was obtained at a mixture ratio of $Ar:N_2 = 200:1$. At pressures higher than 300 torr, the discharge in the Ar- N_2 mixtures was constricted or was not ignited at all. The radiation characteristic in air and nitrogen differed but slightly. At the voltage amplitude of 12.5 kV and its rise time of 200 ps, the average UV power in the Ar- N_2 mixture was 5.8 mW at a radiation efficiency of 1.28% to the angle 4π .

The least radiation pulse width $\tau_{1/2}$ (~ 200 ns) was found in barrier discharges in air and nitrogen (Fig. 5b). However, this width was much longer than the voltage pulse width of the FPG-10 generator. In nitrogen, the radiation pulse width decreased until the pressure reached 30 torr, whereupon it increased slightly. This can be associated with a change in the discharge characteristics. In the $Ar:N_2 = 50:1$ mixture at a pressure of 180 torr, the radiation pulse width of the N_2 -excilamp was 210 ns. In the radiation spectrum of the Ar- N_2 mixture, most of the radiation energy is concentrated in the second positive nitrogen system in which the highest intensity belongs to the band with $\lambda = 337.1$ nm. On excitation of xenon, the gap was broken down at a pressure lower than ~ 10 torr, and this led to a very low radiation efficiency of xenon dimers at 172 nm.

3.4. Short-pulse light sources driven by runaway electron preionized diffuse discharge

To create gas discharge emitters with a pulse width of several nanoseconds, we used a runaway electron preionized diffuse discharge (REP DD). The electrodes of small curvature radius provide electric field amplification, and this ensures the generation of runaway electrons and X-rays, preionization of the discharge gap, and diffuse character of discharges in gases at increased pressures. The use of voltage pulses with a rise time of hundreds of picoseconds increases the efficiency of generation of runaway electrons [13].

It is found that on excitation by the FPG-10 generator at a voltage pulse rise time of 200 ps, a diffuse discharge in the form of a cylinder of height 3 mm and diameter ~ 1 mm is formed between two pointed metal electrodes spaced by 3 mm at atmospheric pressure of air and nitrogen (Fig. 6a).

Under these conditions, the FWHM of the radiation pulse $\tau_{0.5}$ was 3 ns, and the average UV radiation power to the solid angle 4π was 3.5 mW.

As the interelectrode gap was decreased, the discharge became constricted and transformed into a spark. However, even at an interelectrode gap of ~ 0.5 mm, the discharge first assumed the volume form and then transformed to a spark. This is clearly seen in comparing Figs. 6b and 6c which show photos of the discharge taken with

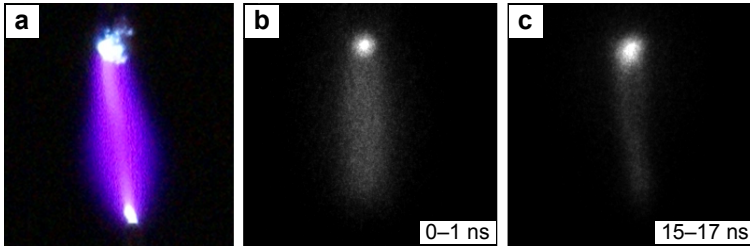


Fig. 6. Integral photo of the discharge (a) taken in a pulse with an interelectrode gap of 2 mm and its photos at different points in time (b, c) with an interelectrode gap of 0.5 mm.

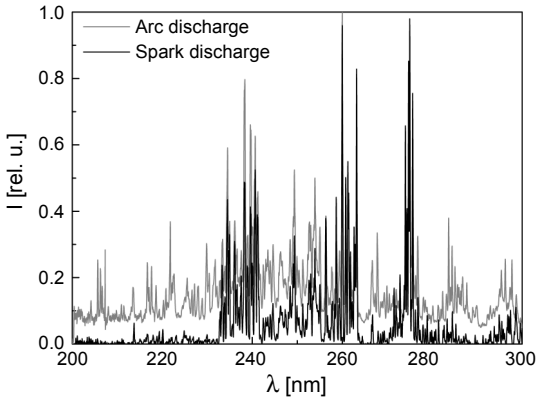


Fig. 7. Radiation spectra of the spark and arc discharges with stainless steel electrodes at 200–300 nm.

a CCD camera at different points in time. The FWHM of the radiation pulse in the spark discharge at a gap of 0.5 mm was ~ 70 ns. The radiation spectrum of the discharge was also studied at gaps of 3, 2, 1, and 0.5 mm. At a gap of 3 and 2 mm, the radiation spectrum of the diffuse discharge was dominated by bands of the second positive nitrogen system, like in [18]. As the gap was decreased from 2 to 0.5 mm, the discharge spectrum changed: radiation of continuum in the wavelength region of 200–450 nm and additional spectral lines of metals in the wavelength region of 700–850 nm, along with the second positive nitrogen system, appeared in the spectrum. In this case, the radiation power of the second positive nitrogen system was almost unchanged, and the power of broadband radiation and metal lines was increased substantially. The radiation energy at 200–300 nm was $\sim 40\%$ of the total energy in the spectral range under study (200–850 nm). Figure 7 shows the radiation spectrum of the spark discharge ($d = 0.5$ mm) and the radiation spectrum of Fe in an arc discharge for comparison. Most of the lines in the spark spectrum coincide with the spectral lines of Fe. This suggests that the lines in the spark spectrum correspond to the lines of vapors of the electrode material; in this case, to iron. At an interelectrode gap $d = 1$ mm, the energy concentrated in the continuum and spectral lines of Fe is lower than that at an interelectrode gap of $d = 0.5$ mm; that is, this case is intermediate in going from $d = 2$ mm

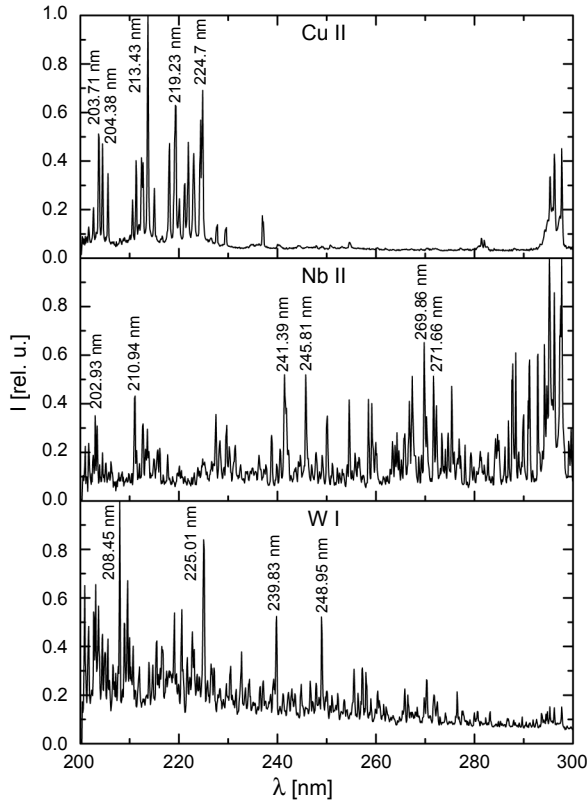


Fig. 8. Radiation spectra of the discharge with copper, niobium, and tungsten electrodes at $d = 0.5$ mm.

to $d = 0.5$ mm. The most interesting results were obtained with electrodes made of copper, niobium, and tungsten. The spectra for these electrodes are shown in Fig. 8. It is seen that the radiation of the discharge with the above electrodes contains lines of neutral atoms and lines of ions of these materials. In the experiments, it was found that with a gap of 0.5 mm, weak X-ray radiation propagated from the discharge gap. This radiation was detected with the scintillation detector. The presence of X-rays from the discharge gap owes to bremsstrahlung radiation of runaway electrons arising early in the formation of the discharge and providing conditions for its diffuse operation.

4. Conclusions

Based on a barrier discharge, the compact sealed-off emitters with UV power densities comparable with those of commercial deuterium lamps were designed. The radiation spectrum of coplanar excilamps differs from the spectrum of conventional DBD excilamps by the presence of a $C-A$ transition band, and from that of capacitive and glow discharge excilamps, by concentration of most of the power in the narrower $B-X$ transition band. In the single-barrier discharge in Ar:N_2 the energy characteristics of

UV radiation are the same but the radiation pulse width is shorter and is hundreds of nanoseconds. The spectral characteristics of the REP DD in atmospheric pressure air were studied. It is shown that this type of discharge can be used in designing compact emitters with nanoseconds radiation pulse duration whose radiation spectrum in individual regions can be varied due to the use of different electrode materials.

References

- [1] KOGELSCHATZ U., *Dielectric-barrier discharges: their history, discharge physics, and industrial applications*, Plasma Chemistry and Plasma Processing **23**(1), 2003, pp. 1–46.
- [2] MILDREN R.P., CARMAN R.J., *Enhanced performance of a dielectric barrier discharge lamp using short-pulsed excitation*, Journal of Physics D: Applied Physics **34**(1), 2001, pp. L1–L6.
- [3] JUN-YING ZHANG, BOYD I.W., *Efficient excimer ultraviolet sources from a dielectric barrier discharge in rare-gas/halogen mixtures*, Journal of Applied Physics **80**(2), 1996, pp. 633–638.
- [4] LOMAEV M.I., SKAKUN V.S., SOSNIN E.A., TARASENKO V.F., SHITTS D.V., EROFEEV M.V., *Excilamps: efficient sources of spontaneous UV and VUV radiation*, Physics–Uspekhi **46**(2), 2003, pp. 193–209.
- [5] KOGELSCHATZ U., ESROM H., ZHANG J.-Y., BOYD I.W., *High-intensity sources of incoherent UV and VUV excimer radiation for low-temperature materials processing*, Applied Surface Science **168**(1–4), 2000, pp. 29–36.
- [6] TODE M., TAKIGAWA Y., IGUCHI T., MATSUURA H., OHMUKAI M., SASAKI W., *Removal of carbon contamination on Si wafers with an excimer lamp*, Metallurgical and Materials Transactions A **38**(3), 2007, pp. 596–598.
- [7] BOYD I.W., ZHANG J.Y., KOGELSCHATZ U., *Photo-Excited Process, Diagnostics and Application*, Kluwer Academic Publishers, The Netherlands, 2003, pp. 161–199.
- [8] EROFEEV M.V., KIEFT I.E., SOSNIN E.A., STOFFELS E., *UV excimer lamp irradiation of fibroblasts: the influence on antioxidant homeostasis*, IEEE Transactions on Plasma Science **34**(4), 2006, pp. 1359–1364.
- [9] STOFFELS E., KIEFT I.E., SLADEK R.E.J., VAN DEN BEDEM L.J.M., VAN DER LAAN E.P., STEINBUCH M., *Plasma needle for in vivo medical treatment: recent developments and perspectives*, Plasma Sources Science and Technology **15**(4), 2006, pp. S169–S180.
- [10] MÜHLBERGER F., WIESER J., ULRICH A., ZIMMERMANN R., *Single photon ionization (SPI) via incoherent VUV-excimer light: robust and compact time-of-flight mass spectrometer for on-line, real-time process gas analysis*, Analytical Chemistry **74**(15), 2002, pp. 3790–3801.
- [11] YUBERO C., GARCÍA M.C., CALZADA M.D., *Using a halogen lamp to calibrate an optical system for UV-VIS radiation detection*, Optica Applicata **38**(2), 2008, pp. 353–363.
- [12] NOGGLE R.C., KRIDER E.P., WAYLAND J.R., *A search for X-rays from helium and air discharge at atmospheric pressure*, Journal of Applied Physics **39**(10), 1968, pp. 4746–4748.
- [13] TARASENKO V.F., BAKSHT E.KH., BURACHENKO A.G., KOSTYRYA I.D., LOMAEV M.I., RYBKA D.V., *High-pressure runaway-electron-preionized diffuse discharges in a nonuniform electric field*, Journal of Technical Physics **55**(2), 2010, pp. 210–218.
- [14] TARASENKO V.F., YAKOVLENKO S.I., *The electron runaway mechanism in dense gases and the production of high-power subnanosecond electron beams*, Physics–Uspekhi **47**(9), 2004, pp. 887–905.
- [15] BAKSHT E.H., BURACHENKO A.G., KOSTYRYA I.D., LOMAEV M.I., RYBKA D.V., SHULEPOV M.A., TARASENKO V.F., *Runaway-electron-preionized diffuse discharge at atmospheric pressure and its application*, Journal of Physics D: Applied Physics **42**(18), 2009, article 185201.
- [16] LOMAEV M.I., MESYATS G.A., RYBKA D.V., TARASENKO V.F., BAKSHT E.KH., *High-power short-pulse xenon dimer spontaneous radiation source*, Quantum Electronics **37**(6), 2007, pp. 595–596.
- [17] EROFEEV M.V., TARASENKO V.F., *Study of a volume discharge in inert-gas halides without preionisation*, Quantum Electronics **38**(4), 2008, pp. 401–403.

- [18] ZAGULOV F.YA., KOTOV A.S., SHPAK V.G., YURIKE YA.YA., M.I. YALANDIN, *RADAN – a small-sized pulsed-repeating high-current electron accelerator*, *Pribory i Tekhnika Eksperimenta* **2**, 1989, pp. 146–149.
- [19] EROFEEV M.V., TARASENKO V.F., *XeCl-, KrCl-, XeBr- and KrBr-excimer lamps of the barrier discharge with the nanosecond pulse duration of radiation*, *Journal of Physics D: Applied Physics* **39**(16), 2006, pp. 3609–3614.
- [20] TAO SHAO, TARASENKO V.F., CHENG ZHANG, BAKSHT E.KH., PING YAN, SHUTKO Y.V., *Repetitive nanosecond-pulse discharge in a highly nonuniform electric field in atmospheric air: X-ray emission and runaway electron generation*, *Laser and Particle Beams* **30**(3), 2012, pp. 369–378.
- [21] JINZHOU XU, YING GUO, LEI XIA, JING ZHANG, *Discharge transitions between glow-like and filamentary in a xenon/chlorine-filled barrier discharge lamp*, *Plasma Sources Science and Technology* **16**(3), 2007, pp. 448–453.
- [22] TARASENKO V.F., CHERNOV E.B., EROFEEV M.V., LOMAEV M.I., PANCHENKO A.N., SKAKUN V.S., SOSNIN E.A., SHITZ D.V., *UV and VUV excimer lamps excited by glow, barrier and capacitive discharges*, *Applied Physics A: Materials Science and Processing* **69**(1 Supplement), 1999, pp. S327–S329.
- [23] SOSNIN E.A., EROFEEV M.V., TARASENKO V.F., *Capacitive discharge excimer lamps*, *Journal of Physics D: Applied Physics* **38**(17), 2005, pp. 3194–3201.
- [24] FALKENSTEIN Z., COOGAN J.J., *The development of a silent discharge-driven XeBr* excimer UV light source*, *Journal of Physics D: Applied Physics* **30**(19), 1997, pp. 2704–2710.
- [25] BABICHEV A.P., *Reference Book on Physical Values*, [Eds.] Grigor'ev I.S., Meilikhov E.Z., Energoatomizdat, Moscow, 1991, (in Russian).
- [26] KOGELSCHATZ U., *Silent discharges for the generation of ultraviolet and vacuum ultraviolet excimer radiation*, *Pure and Applied Chemistry* **62**(9), 1990, pp. 1667–1674.
- [27] ROTH J.R., *Industrial Plasma Engineering*, Vol. 1, IOP, Bristol, UK, 1995, p. 420.
- [28] LOMAEV M.I., TARASENKO V.F., TKACHEV A.N., SHITTS D.V., YAKOVLENKO S.I., *Formation of coniform microdischarges in KrCl and XeCl excimer lamps*, *Technical Physics* **49**(6), 2004, pp. 790–794.
- [29] MARCHAL F., SEWRAJ N., JABBOUR G., RODRIGUEZ AKERRETA P., LEDRU G., *Temperature dependence of xenon excimer formations using two-photon absorption laser-induced fluorescence*, *Journal of Physics B: Atomic, Molecular and Optical Physics* **43**(23), 2010, article 235210.

Received May 16, 2014
in revised form June 26, 2014